Chapter 1

Compiling single sections at a time

For writing purposes only.

Chapter 2

Theory Part II (need to rename)

Describe analytical models, numerical models (omega), simulations (eris) and that I compare the two latter Results from omega can be compared to hydrodynamical simulations like eris. Which are much more detialed and precise, but also more computationally expensive.

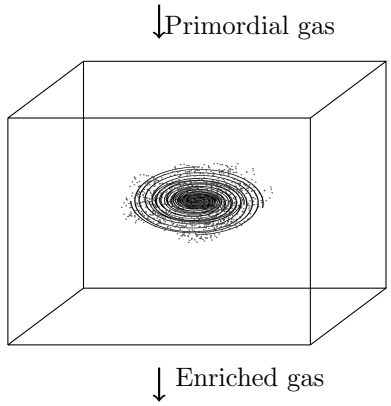

Figure 2.1

2.1 The Omega model

Omega is a python code developed by Benoit Côté and Christian Ritter[1]. OMEGA stands for 'One-zone Model of the Evolution of Galaxies' and evolves the isotopic content of a galaxy *(Côté et al., 2016)* . The model is a one-zone model, which means that the entire galaxy is simplified to a single point. A zero-space-dimensional galaxy model seems unrealistic, but it can be imagined as the mean value for a three-space-dimensional galaxy model.

In this work the Omega code will be modified with a wrapper in order to explore various parameters related to nucleosynthesis.

2.1.1 Process

The Omega model emulates the chemical evolution of a galaxy starting from the initial primordial gas. A simple stellar population is created by integrating the star formation rate over time. The star formation rate is calculated either by using a constant star formation rate, the Kennicut-Schmidt law *(Fuchs et al., 2009, and refernces therein)* , or by using an input star formation rate and interpolate over those values.

The stellar populations represent a cluster of stars, with a total mass, initial mass distribution, and initial metallicity distribution. The initial mass distributions are given as one of the standard distributions, Salpeter, Kroupa, Chabrier, or a power-law, all between some minimum and maximum mass limit (see figure 2.2. The initial metallicity distribution is the relative mass distribution of isotopes heavier than $^{7}_{3}\mathrm{Li}$, and the metallicity is the mass fraction of all isotopes heavier than $^{7}_{3}\mathrm{Li}$ combined.

Stellar evolution codes calculate the amount of ejected material, for each isotope, for a star with a given initial metallicity and initial mass. These codes are used to create **yield tables** for certain kind of stars with different initial mass and metallicity.

In the simple stellar population assumed in the galactic chemical evolution model,

[1] https://nugrid.github.io/NuPyCEE/

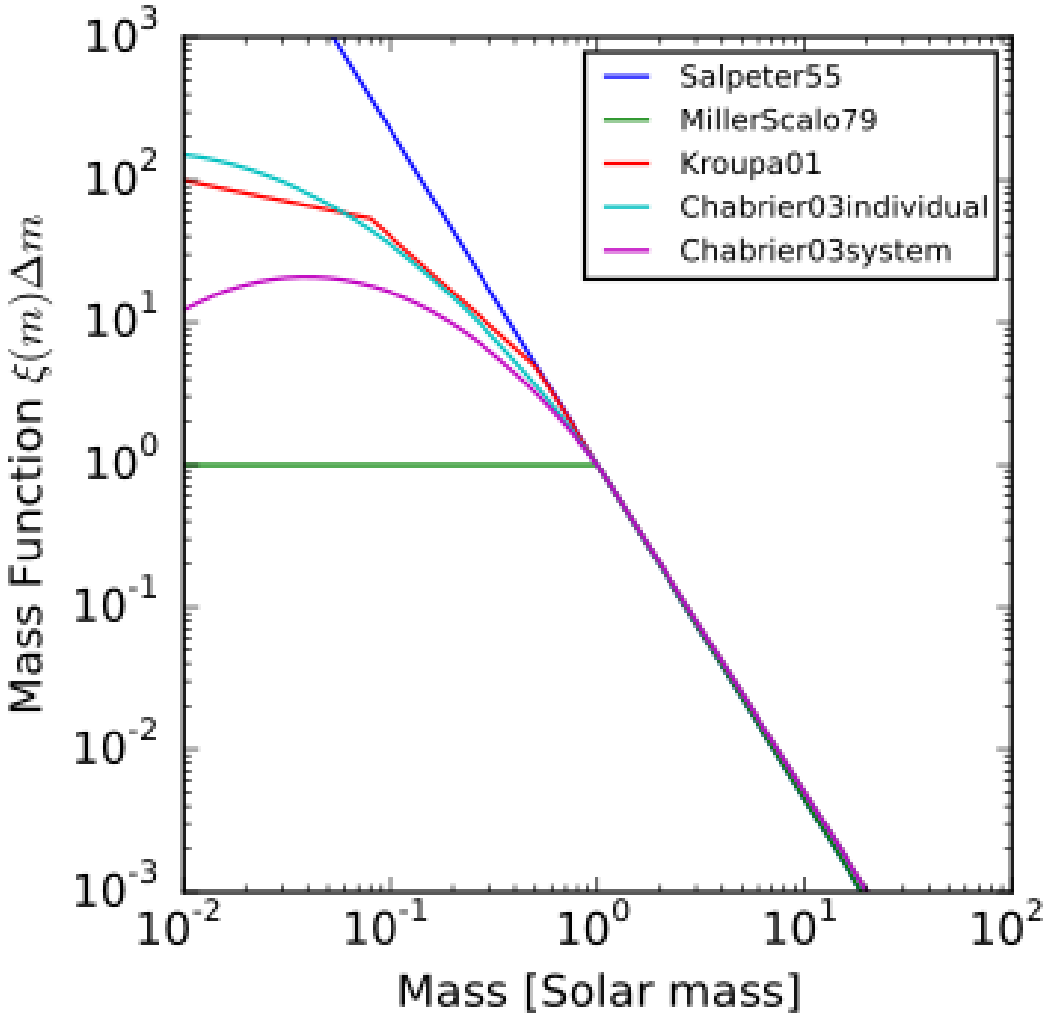

Figure 2.2: A simplified visualization of some of the common initial mass functions in the literature. *(Cappellari et al., 2012, and references therein)* , *(Salpeter, 1955)* , *(Kroupa, 2001)* , *(Chabrier, 2003)* , *(Miller & Scalo, 1979)* .
image-credit: By JohannesBuchner [CC BY-SA 4.0 (`https://creativecommons.org/licenses/by-sa/4.0`)], from Wikimedia Commons

these yield tables are used to calculate the chemical composition and mass of ejecta from each group of stars. The ejecta are disspersed back into the interstellar medium (gas of the galaxy model) at delay-times appropriate for each group of stellar mass. E.g. For a given mass-bin the total mass in stars, number, and age of stars, with initial mass in that bin, are calculated using the total mass of the total stellar mass and mass function chosen. By choosing the yield tables closest in initial mass and initial metallicity the total ejecta composition is calculated and added to the interstellar medium at the age where those stars would have gone supernova. The material that is not ejected is left as remnants and total mass and number of remnants are also added to the simulation at the time these stars would have gone supernova.

In `Omega` the creation and treatment of simple stellar population is done by another python-program called `Sygma`.

The `Omega` model is a *one-zone* model, meaning that everything inside the box has been enriched from stellar lifecycles. Everything outside the box is untouched since "it's creation", and has the same composition as the material inside the box had to start with. This composition is called the primordial composition (three parts hydrogen, one part helium and trace amounts of lithium and beryllium), and is derived from the big bang nucleosynthesis (see section**??**. Flow of material can determine the chemical evolution of a galaxy. Enriched material can be ejected from the galaxy by supernova feedback, active galactic nucleus, stellar kick or similar, and non-enriched material can flow into the galaxy. To describe the chemical evolution of a one-zone model one needs to know the total content of the galaxy (or box) and the distribution. In other words, how much of the total mass is stored as each isotope. Material with the same composition as the box is ejected from the box, and material with another composition falls into the box.

More on outflow/inflow

Insert simple figure here

2.1.2 Uncertainty of parameters

uncertainty of parameters and summary of article (cote16a)

Galaxies consist of many different, widely varying, scales for both spatial and temporal resolution. The galaxies themselves span hydrodynamical evolution on many kpcs and Gyrs, while their stars and supernovae span scales closer to seconds and meters. The nuclear processes within stars span nanometer and millisecond timescales, even though stars can last for billion years(with short timescale bursts in between). Neither analytical/numerical models nor simulations cannot cover all these scales at once, that is when subgrid methods are used. Stellar evolution simulations predict the fate and output from the life of a single star based on sinple input parameters and assumptions of the physical processes that governs the evolution. These solutions are then simplified and applied to more complex galaxy simulations. Output ejecta from stars are "looked up in a table" and applied to the nearby interstellar medium. All these methods and linked applications introduce some uncertainties and assumptions, both physical and numerical, and these uncertainties are inherited through all methods based on applica-

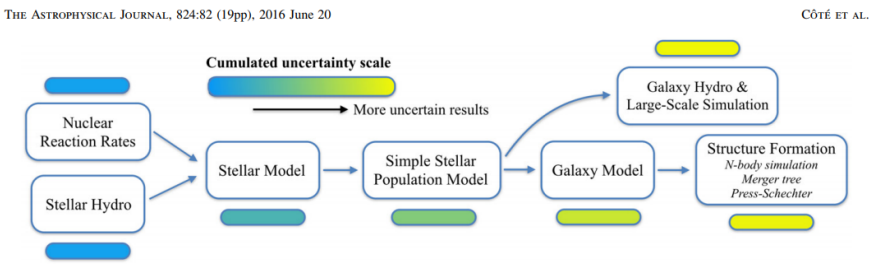

Figure 2.3: Qualitative visualization of how uncertainties accumulate in galactic chemical evolution models. Experimental data on nuclear reaction rates are uncertain to some degree. The change in rate and uncertainty in stellar conditions are not well known. The conditions inside a star of a given mass and metallicity come from 1 dimensional hydrodynamical simulations. The combined result from nuclear reactions and hydrodynamical simulations give a stellar models. The stellar models are applied to a simple stellar population to account for all the billions of stars in galaxy. These stellar models are then applied to a large scale hydrodynamical simulation (like `Eris`), or a semianalytical galaxy model (like `Omega`). All the steps make assumptions and add uncertainty to the grand total uncertainty that is difficult to map in completeness.
Diagram is taken from *(Côté et al., 2016, fig.1)*

tions of these models. In order to probe how the uncertainties of selected parameters manifest through the resulting galaxy evolution, *(Côté et al., 2016)* presents a simple one-zone, closed-box model of galaxy evolution, called `Omega`.

`Sygma`creates the simplified stellar populations (mass function, total mass, lifetime distribution, initial metallicity). `Omega` combines several stellar populations to emulate a galaxy evolution.

Stellar yields are tables from stellar evolution simulations. The tables used in `Omega`are taken from, among other sources, NuGrid[2] and include AGB stars between 1 and 7 $M_{\odot}$, massive stars between 12 and 25 $M_{\odot}$, all with metallicities at $Z = 0.02, 0.01, 0.006, 0.001, 0.0001$. These tables contain many isotopes between hydrogen and bismuth.

The stellar evolution was calculated with MESA[3], post-processing was done with MPPNP *(Hirschi et al., 2008)* , the same nuclear reaction rates were used in all calculations, explosive nucleosynthesis was done with semi-analytical models. Yields are complemeted with SN1a yields from *(Seitenzahl et al., 2013)* , *(Thielemann et al., 2003)* , *(Iwamoto et al., 1999)* , *(Thielemann et al., 1986)* and population III yields from *(Heger & Woosley, 2010)* (other sources are available from the literature, but these are the focus of the chemical evolution of this thesis. Sources for neutron star mergers will be discussed later).

The probability distribution functions for the input parameters are created from

[2]NuGrid collaboration: Homepage Github

[3]MESA is a modular, opensource code to evolve single star systems, and can do so from main sequence to white dwarf stage or core collapse stage. See Homepage for further information

values and uncertainties in the literature. Methodologically there are, for each input parameter, gathered a list of literature values and uncertainties. The errors are considered gaussian in nature and distributions are created thereafter, all the distributions are then averaged to a single distribution. Then a single gaussian is fitted atop the "average of gaussians from the literature", and the median and standard deviation from the final fit is used as value and uncertainty for the input parameter in question.

(Côté et al., 2016) sampled a set calculations, for each parameter in figure 2.4 a series of 300 calculations were made with a random sampling of the input parameter for the gaussian uncertainty distribution. A set of 700 calculations were made were all the input parameters were all the input parameters were randomly drawn from their respective gaussian distributions. An additional 300 calculations were made with the final gas-mass and final stellar mass both drawn randomly from their respective gausssian distributions.

Spectroscopic abundance of metals are measured in [X/Y] where X is the metal in question and Y is the reference metal, either plotted against metallicity, [Y/H], or galactic time, Gyr.

The main conclusions are summarized as follows:

1. The overall uncertainty of spectroscopic metals between 0 and 0.6 dex when plotted against metallicity, but the uncertainty is higher when considered against galactic time.

2. - Ratio of final mass of gas to final mass of stars affect the uncertianty for early times ([Fe/H] $\lesssim$ -2) since more gas means more hydrogen, while more stars means more iron-production. Since metals are also produced in stars, the ratio does not affect [X/fe] much.
   - Number of type 1a supernovae and their delay time distribution affect the uncertainty of spectroscopic metals at later times([Fe/H] $\gtrsim$ -1.5 $\rightarrow$ t $\gtrsim$ 150Myr), when the delay-time has allowed for type 1a supernovae to occur. Type 1a supernovae add mostly iron to the interstellar medium, while not producing much of metals produced by AGB stars and massive stars. This means that the uncertainty of [X/Fe] will be greatly affected by uncertianties in type 1a supernovae.
   - The high mass slope of the initial mass function, α, determines the ratio of massive stars to low-mass stars at all times. Massive stars die quickly and distributed much enriched material into the interstellar medium. Therefor the uncertainty of the slope will always be prevailent in the uncertainty of spectroscopic metals.
   - Uncertainties in the mass ranges of the initial mass function does not affect uncertainties of the spectroscopic abundances much.

3. Uncertainties in the slope of the initial mass function, α, and the number of type 1a supernovae affect the uncertainties in the spectroscopic abundances. When plotted against metallicity ([Fe/H]) the uncertainty is greatest when the considered metal and the reference metal is not from the same source.

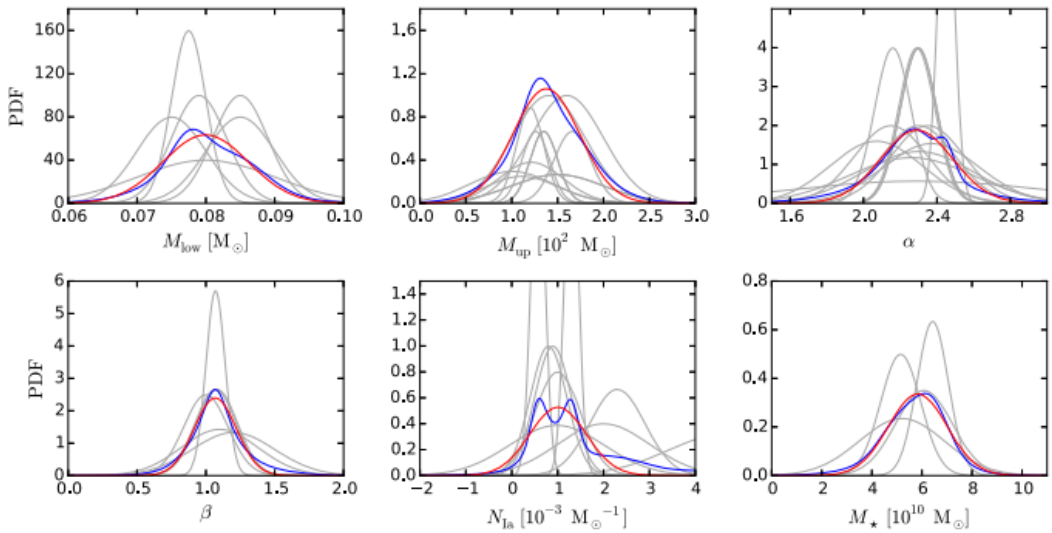

Table 7
List of the Seven Input Parameters Used in this Work to Generate Uncertainties in Our Numerical Predictions

Parameter	Description	Typical value	Reference
	Simple Stellar Population		
$M_{\rm low}$	Lower mass limit of the IMF [$10^{-2}\,M_\odot$]	8.00 ± 0.62	Table 1
$M_{\rm up}$	Upper mass limit of the IMF [$M_\odot$]	138 ± 36	Table 2
α	Slope of the IMF	2.29 ± 0.20	Table 3
β	Slope of the DTD of SNe Ia	1.07 ± 0.15	Table 4
$N_{\rm Ia}$	Number of SNe Ia [10^{-3} M$_\odot^{-1}$]	1.01 ± 0.62	Table 5
	Galaxy		
$M_{\star,f}$	Current stellar mass[a] [$10^{10}\,M_\odot$]	5.84 ± 1.17	Table 6
$M_{\rm gas,f}$	Current mass of gas[b] [$10^9\,M_\odot$]	9.2 ± 5.3	Kubryk et al. (2015)

Notes. The value and uncertainty of each parameter are the mean value and the standard deviation taken from the corresponding Gaussian fit presented in Figure 2.
[a] This parameter is used to calibrate the SFH (see Section 3.6).
[b] This parameter is used to derive the initial mass of gas (see Equation (8)).

Figure 2.4: How the input parameters were determined from multiple sources in the literature. Values and standard deviations averaged to a probaiblity distribution, and then fitted to a single gaussian distribution. Images from *(Côté et al., 2016, figure 2 and table 7)* .

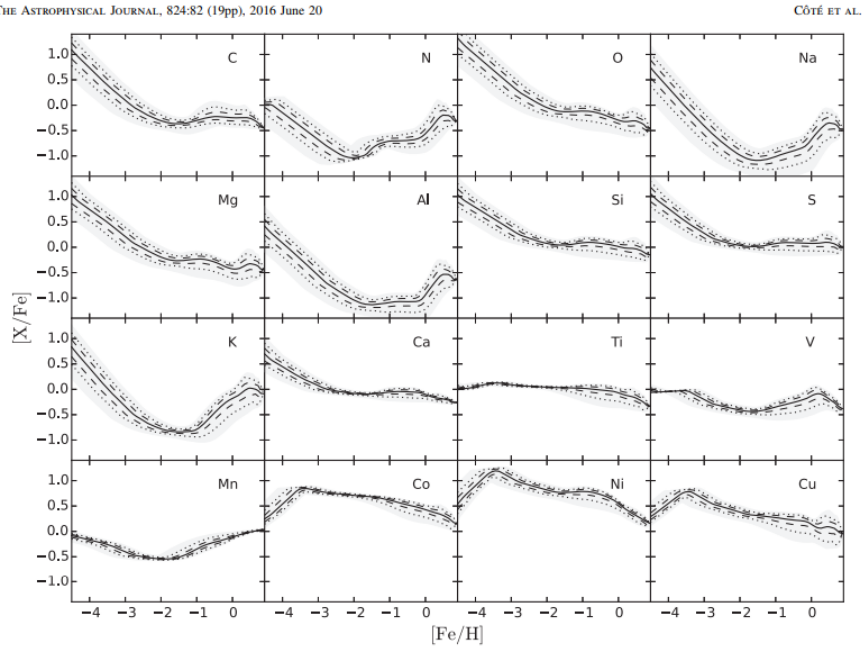

Figure 2.5: Spectroscopic abundance of 16 metals relative to iron, considering uncertainties of all parameters (upper bound, lower bound and high mass slope of initial mass function, stellar and gas mass today, number of type 1a supernovae and the slope of the type 1a supernova delay-time distribution).
Plots and figures are taken from *(Côté et al., 2016, fig.6)*

4. The characteristics seen from spectroscopic abundance against metallicity is shared regardless of the introduced uncertainties. The introduced uncertainties amplify the characterstic shapes, but do not change them. "Such features are mainly caused by the choice of stellar yields and the type of galaxy considered." *(Côté et al., 2016, p.18)*

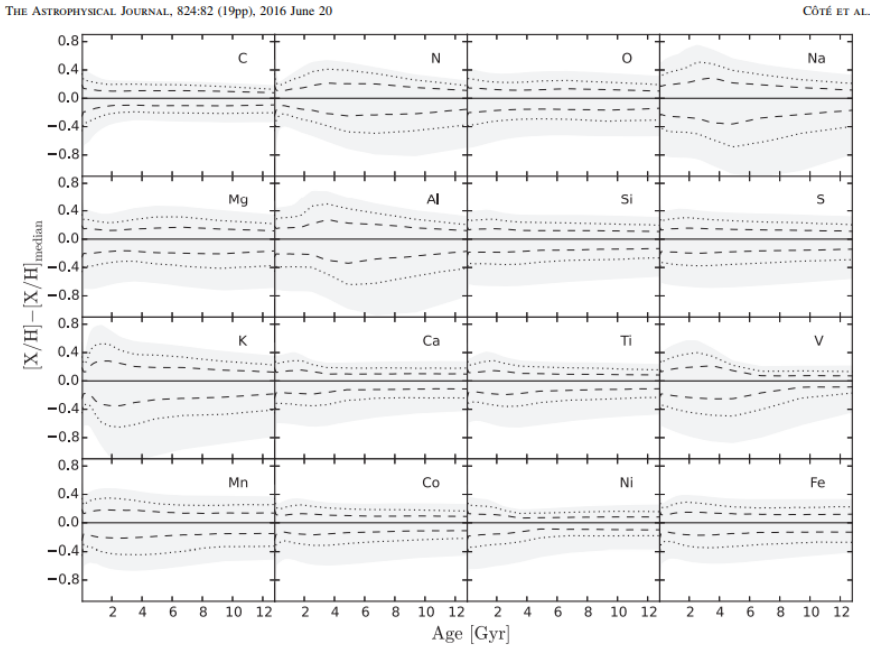

Figure 2.6: Uncertainty of spectroscopic abundance of 16 metals relative to iron, considering uncertainties of all parameters (upper bound, lower bound and high mass slope of initial mass function, stellar and gas mass today, number of type 1a supernovae and the slope of the type 1a supernova delay-time distribution).
Uncertainties relative to mean shown as a function of galactic age.
Plots and figures are taken from *(Côté et al., 2016, fig.6)*

2.1.3 Relevant parameters

`Omega` has many input parameters, both numerical and physical in nature, to guide the evolution of the galaxy. A physical input parameters are model parameters, while a numerical parameter decides on which calculations to choose from and where to get data. E.g initial gas of galaxy is considered physical, while the boolean switch to turn on neutron star mergers are considered numerical

This section will describe the most relevant ones in order of appearance in the program.

galaxy This string option chooses predefined parameters to best match a certain galaxy on record. The relevant options are:

None No parameters determined.

milky_way_cte Set present dark matter mass to $10^{12} M_\odot$ and present stellar mass to $5 \times 10^{10} M_\odot$, and use a constant star formation rate of $1 \frac{M_\odot}{yr}$

milky_way Set present dark matter mass to $10^{12} M_\odot$ and present stellar mass to $5 \times 10^{10} M_\odot$, and use the star formation rate from *(Chiappini et al., 2001)*

in_out_control Boolean switch to turn on or off inflow and outflow.

outflow_rate remove this? Constant outflow rate in $\frac{M_\odot}{yr}$. Enriched gas from the interstellar medium is removed from the galaxy.

inflow_rate Constant inflow rate in $\frac{M_\odot}{yr}$. Gas with primordial composition (reference to BBN?) flows into the galaxy.

mass_loading Fraction of solar masses ejected per solar mass created as star. A different way of calculating outflow based on star formation rate.

imf_type Which form to use for the initial mass function explain this somewhere .

alphaimf Slope of lognormal initial mass function.

sn1a_rate This string option chooses which distribution to calculate the rate of type 1a supernovaefrom. Options are powerlaw, gaussian, and exponential distribution.

beta_pow Set the power of the power law distribution if 'sn1a_rate' is "power_law"

gauss_dtd Set the mean and standard deviation of the gaussian distribution if 'sn1a_rate' is "gauss"

exp_dtd Set the e-folding time of the exponential distribution if 'sn1a_rate' is "exp"

dt Length of first timestep (in yrs)

special_timesteps Number of logarithmic timesteps

tend Final point in time (in yrs)

mgal Initial mass of gas (if not calculated by other means), defaults to $10^{10} M_{\odot}$

transitionmass=8 Mass-limit that separates the AGB stars from the massive stars explain these stars somewhere . Defaults to $8 M_{\odot}$

nb_nsm_per_m Set the number of neutron star mergers per solar mass formed as stars.

t_nsm_coal Set the time after which all neutron stars collide/merge

table path to yield table for AGB and massive stars.

sn1a_on Boolean switch that turn on or off the use of type 1a supernovae.

nsm_dtd_power Set the powerlaw distribution of the neutron star merger delay-time distribution explain this somewhere .

sn1a_table Yield table for type 1a supernovae

ns_merger_on Boolean switch to turn on or off binary neutron star mergers

f_merger Fraction of binary systems that eventually merge. All systems are considered binary. This is instead of 'nb_nsm_per_m'

m_ej_nsm solar masses ejected per neutron star merger.

nsmerger_table Yield table of binary neutron star mergers

bhns_merger_on Boolean switch to turn on or off black hole neutron star mergers

pop3_table Yield tables for population III stars

imf_bdys_pop3 The boundaries of the initial mass function of population III stars.

nb_1a_per_m The number of type 1a supernovae per solar mass formed. Used to calculate the number of type 1a supernovae from star formation rate.

popIII_on Boolean switch that turn on or off the use of Population III stars

out_follows_E_rate Adds a time-delay to outflow with mass_loading such that outflow follows supernova rate.

sfh_array Two one-dimensional arrays, time and star formation rate, that Omegawill interpolate over in order to find the star formation rate at a given time.

The Astrophysical Journal, 742:76 (10pp), 2011 December 1

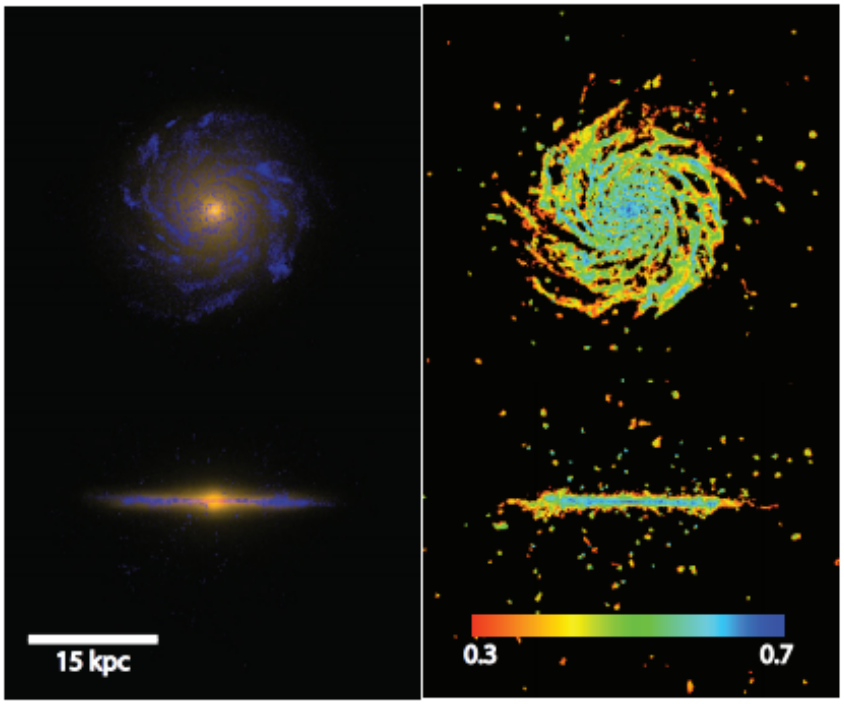

Figure 2.7: *Left panel*: Radiative properties of `Eris` from the stellar composition (assuming a Kroupa initial mass function. *Right panel*: Projected density maps of neutral gas in `Eris`.
Both panels show the galaxy face-on and edge-on. Plots and figures are taken from *(Guedes et al., 2011, fig.2 and references therein)* .

2.2 `Eris` simulation

`Eris` *(Guedes et al., 2011)* is a N-body/smooth particle hydrodynamics simulation of a galaxy forming in ΛCDM cosmology (see section **??**. The simulation is performed with `Gasoline` *(Wadsley et al., 2004)* .

2.2.1 Smoothed particle hydrodynamics

Particle physics can be simulated by calculating the forces acting on each particle, then using newtons second law to get the acceleration of each particle. By integrating in time, with a large variety of numerical methods, the acceleration will give correction to the velocity in the next timestep. In a similar fashion the velocity of each particle will give the position in the next timestep. Examples of such numerical methods are Euler's method, Euler-Cromer's method, Velocity Verlet, Runge-Kutta 4. Numerical particle physics approximates all matter to discrete points in time and space. Due to limited

numerical capabilities, and the sheer scale of astronomical dimensions it will not be able to resolve an entire galaxy. Alternatively to representing a galaxy by many discrete points, is representing a galaxy as a meshgrid of average physical properties. This meshgrid holds physical properties like density, pressure, velocity and internal energy. Flow of mass and energy between the gridspaces is done according to hydrodynamics. Smoothed particle hydrodynamics *(Monaghan, 1992)* represent an effort to combine the two different approaches. Point particles representing a sphere of gas/stars/dark matter with a kernel function to extend the sphere around the point particle. The kernel function is historically represented by a gaussian, but for numerical ease modern methods use a spline-function that is zero outside a given range. Hydrodynamical effects on a particle from another nearby particle is given by the overlapping kernel functions, which represent a higher density/pressure/internal energy region. The hydrodynamical equations then govern change in velocity and temperature.

Gravity and acceleration is calculated in `Gasoline` by solving the Poisson's equation (eq.2.1) and Newton's laws (eq.2.2) for each body. ϕ is the gravitational potential, G is the gravitational constant, ρ is the mass density, a_i is the acceleration on body i, M_j is the mass of body j, $r_i - r_j$ is the distance between body j and i.

$$\nabla^2\phi = 4\pi G\rho \tag{2.1}$$

$$a_i = \nabla\phi = \sum_{i\neq j} \frac{GM_j}{(r_i - r_j)^2} \tag{2.2}$$

The extension of a single particle is represented by a symmetric kernel function that extends to some smoothing length h, with an associated density of (eq.2.3). m_j is the mass of particle j, with W_{ij} being the kernel function between particles i and j.

$$\rho_i = \sum_{j=1}^{n} m_j W_{ij} \tag{2.3}$$

The acceleration from gas pressure between two nearby particles is given by the momentum equation (eq. 2.4). $\vec{v}$ is the velocity of particle i, P_i is the pressure associated with particle i, and Π_{ij} is the artificial viscosity term between the two particles.

$$\frac{\mathrm{d}\vec{v}_i}{\mathrm{dt}} = -\sum_{j=1}^{n} m_j \left(\frac{P_i}{\rho_i^2} + \frac{P_j}{\rho_j^2} + \Pi_{ij}\right) \nabla_i W_{ij} \tag{2.4}$$

The change in temperature/internal energy for the gas in a particle is given by (eq.2.5). u_i is the internal energy of body i and $\vec{v}_{ij}$ is the relative velocity between the two bodies, i and j.

$$\frac{\mathrm{d}u_i}{\mathrm{dt}} = \frac{P_i}{\rho_i^2} \sum_{j=1}^{n} m_j \vec{v}_{ij} \dot{\nabla}_i W_{ij} \tag{2.5}$$

If a group of bodies is far away from an observer, the sum force of each body is similar to force to the mass-center with a mass equal to the sum of indivdual masses. This is exploited numerically by splitting the point particles into "trees" where the force on one body from a group of smaller bodies far away is given by the distance to the mass-center of said group and the sum of masses. Numerically this is done by

calculating the mass-center of all bodies, then splitting the simulation in two sections with equal number of particles and calculate the mass-center of these two sections. This process is repeated iteratively until a single body/point particle is left. In other words; the "tree" stretches into many "branches" with a single particle at the end of each branch. Nearby particles are also grouped together into "leaves". When calculating the force acting on a single particle one calculates the force from each neighbour, but as the distance increases the mass-center for a large "branch" is used instead of all individual "leaves".

`Gasoline` is a parallelized tree-smoothed-particle-hydrodynamics code that tracks particles with a selfgravitating sphere of density, represented by a kernel function around the particle, extending a certain distance from the particle. The particles are "falling in their own gravity", while "flowing their own medium". The code builds a tree to connect all the particles, in order to calculate gravitational forces more efficiently. The tree is also reproduced to calculate periodic boundary conditions more efficiently.

Particle hydrodynamics is only relevant when two smoothing kernels (representing the extension of gas) overlap. When the edges of two kernels start overlapping, the density and pressure the kernel represent increase causing a repulsive force from the hydrodynamical equations of motion and continuity.

Energy transport in `Gasoline` can follow a wide range of procedures, like adiabatic and isothermal cooling processes, hydrogen/helium cooling processes with ionization fractions in addition to ultraviolet feedback from star formation and cosmic background.

2.2.2 Angular momentum problem

In galactic simulations there is an "angular momentum problem". This refers to baryonic components having much less rotaional spin in simulations than real observations. This failure was believed to arise from friction moving angular momentum from substructures to outer halo when these sub-structures merge causing the cold clumps of gas to fall to the center *(Navarro & Benz, 1991)* . Meaning that cosmological simulation with gas become clumped in the center of halos, instead of forming disks like observed galaxies. The "problem" being not enough angular momentum in the gas. In newer times this problem have been attempted solved with energy injected from supernovae, meaning evolving stars from the gas content to decrease the effect of cooling and removing angular moment from the center of the galaxy. The stars heat the surrounding gas, and the supernovae add kinetic energy to the gas so it is not allowed to cluster too much in the center. In the `Eris`-simulation however, an rotational disk is allowed to form. This is because the high resolution (many particles) combined with the high threshold for star formation centeres the star forming regions in the high density regions. Such compact star formation drives cold gas outflow from the center of the galaxy, removing low angular momentum gas into "higher orbits".

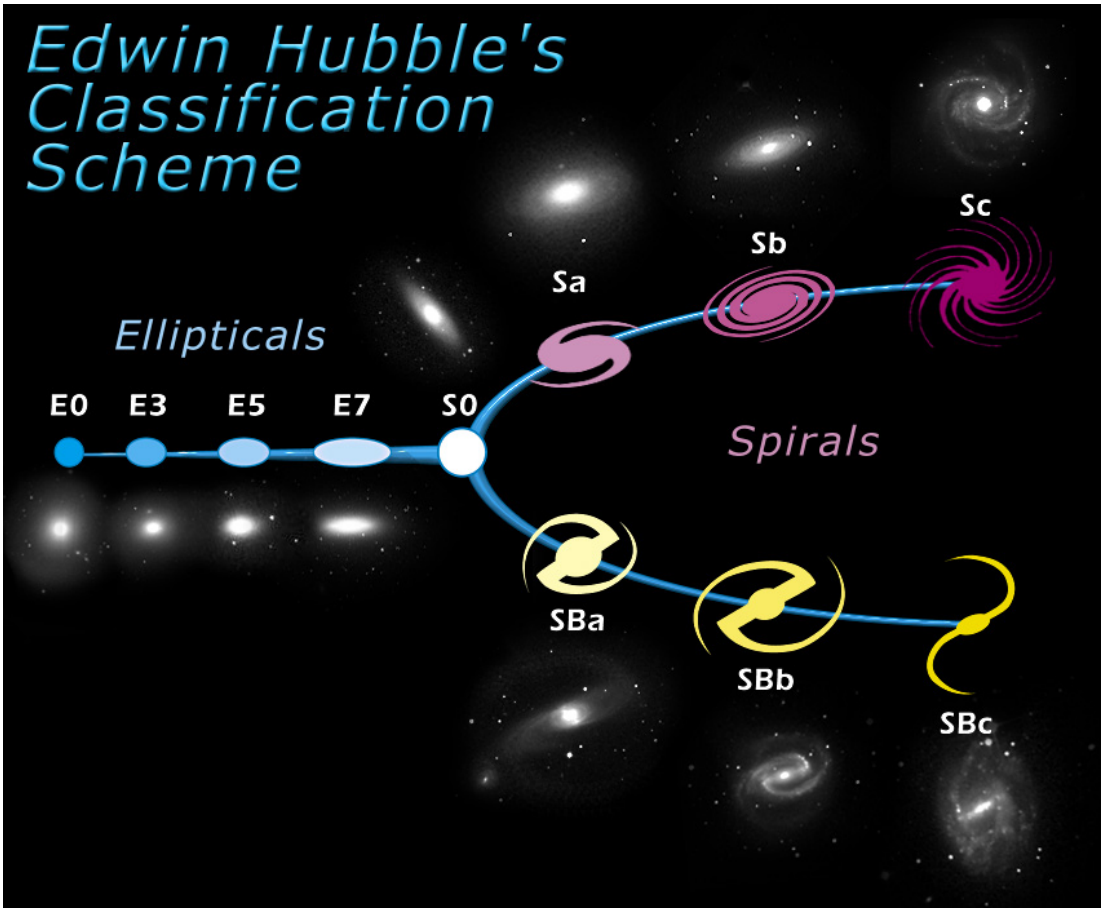

Figure 2.8: **??** The Hubble morphological classification of galaxies from their observed shape. Described either as elliptical, spherical or spherical with a bar in the center. Source: ESA

2.2.3 Properties of the Eris-simulation

The simulation consist of dark matter particles and baryonic gas particles. Star particles are created when the number density passes 5 atoms cm^{-3}[4]. Feedback from an active galactic nucleus is neglected, but supernova-feeback is considered along with cosmic UV background and radiative cooling.

Some properties of the simulated galaxy:

- rotaional disk with scale length $R_d = 2.5kpc$
- "gentle" rotation curve with circular velocities up to 2.2 scale lengths
- i-band (infrared wavelength 806 nm, bandwidth 149 nm) bulge-to-disk-ratio of $B/D = 0.35$
- baryonic mass fraction inside halo is 30% lower then cosmic average
- thin disk with typical HI-stellar mass-ratio
- disk is forming stars in $\Sigma_{sfr} - \Sigma_{HI}$ plane
- disk falls on photometric Tully-Fisher relation and stellar mass - halo virial mass relation
- structural properties, mass budget, and scaling relations between mass and luminosity matches several observational constraints

(Guedes et al., 2011) presents a realistic simulation of a Milky Way type galaxy using a new smooth particle hydrodynamic cosmological simulation called `Eris`, based on `Gasoline` *(Wadsley et al., 2004)* . It includes radiative cooling, cosmic UV heating, supernova feedback, and high-density star formation requirement (which is believed to be a key ingredient in producing realistic spirals in galactic simulations). The high density threshold for star formation (5 atoms cm^{-3}) creates sparsely, clustered regions of star formation that remove low-angular momentum cold gas from the center of the halo.

By using the `Eris`-simulation, the chemical evolution of the milky way is studied. `Eris` traces oxygen and iron from supernovae. *(Shen et al., 2015)* postprocesses the simulation data from `Eris` to include neutron star mergers that add europium (an r-process tracer) to the interstellar medium. The study shows that the heavy products of neutron star mergers can be incorporated into early stars, even if the shortest neutron star mergers is 100 Myr. The conclusion of the study does not vary much with delay-time and merger rate and an argument is made for neutron star mergers being the dominant r-process source in the galaxy.

This is supported by the neutron star merger (GW170817) observed *(Troja et al., 2017)* . With *estimated* dynamical ejecta of mass 0.002 $M_\odot$ and velocity of 0.2c and

[4] Assuming three quarter neutral hydrogen and one quarter neutral helium, by mass, this threshold density equals $0.043 M_\odot pc^{-3}$. A gas particle is initially represented by a total mass of $2 \times 10^4 M_\odot$ and a smoothing length/radius of 120pc.

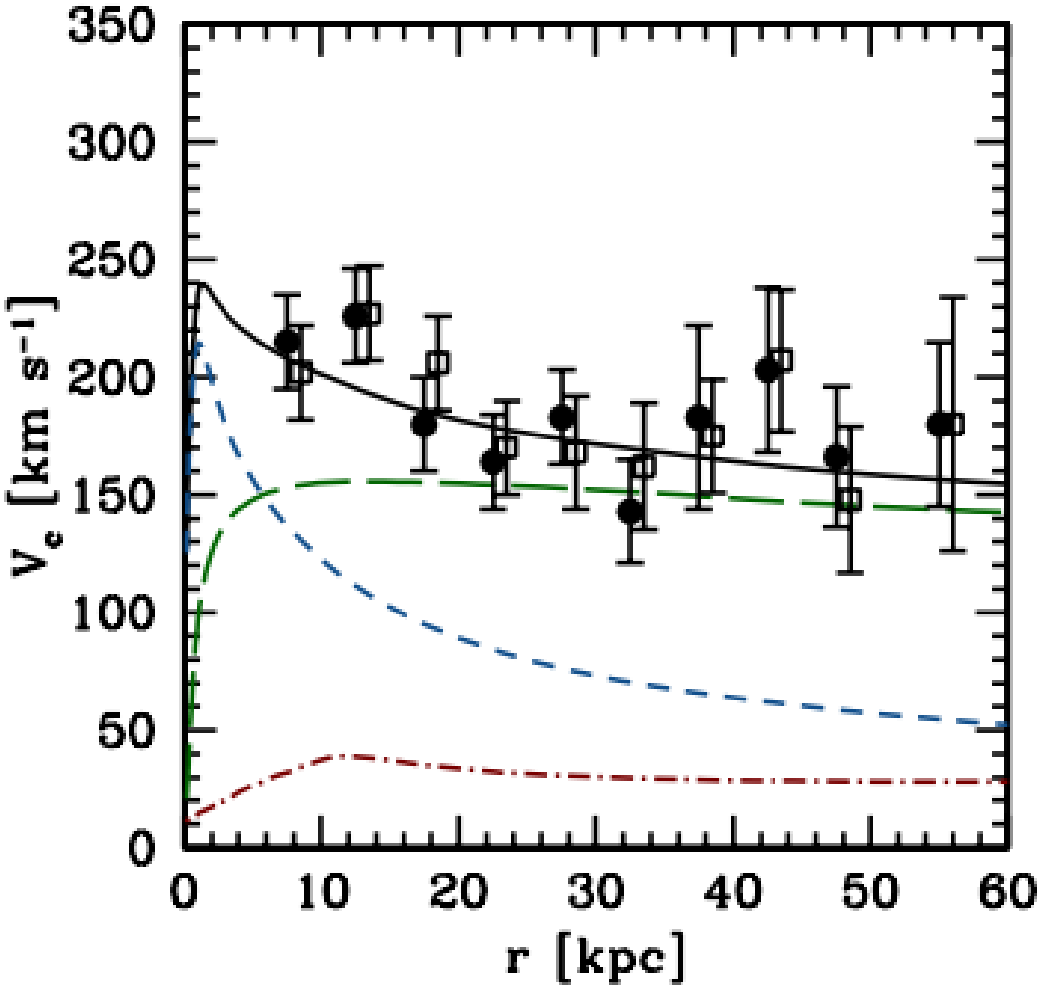

Figure 2.9: Contribution to rotation curve in `Eris` at redshift zero. The circular velocity is calculated as a function of radius, $v_c = \sqrt{GM(< r)/r}$, for the different types of particles. *Red dash-dotted line*; gas within virial radius, *blue short dashed line*; stars, *green long dashed line*; dark matter, *black solid line*; total contribution from all mass in `Eris`, *data points*; *Sloan Digital Sky Survey.*
Plots and figures are taken from *(Guedes et al., 2011, fig.1 and references therein)* .

highspeed wind ejecta of mass 0.015 $M_{\odot}$ and velocity of 0.08c. Such velocities are high enough to cross a galaxy within $\simeq$ 1 Gyr, and if most of the ejecta manifests as r-process material the assumed model of *(Shen et al., 2015)* (ejected r-process material of 0.01 $M_{\odot}$) is realistic. The single GW170817 observation makes rate of such events hard to estimate, and therefore difficult to constrain the neutron star merger rate in `Eris`.

2.2.4 move to theory I

Looking at very metal poor stars in our Galaxy, which have been around for a long time, r-process abundances can be found. Meaning that the source of r-process has been around for a long time, and in a robust manner. However, the large variations show that the process was unhomogenous for early times, while it is more smoothed after many Galactic rotations and repeated events. The two main sources of producing these heavy r-process elements are believed to be in the merger of two neutron stars (or the merger between a neutron star and a black hole) or in a heavy core collapse supernova. The production yields are much larger for neutron star mergers, but they are also much more rare. (Important citations Takashi94 and Woosley94 for SNII; Lattimer 77 and Freiburghaus 99 for NSM)

r-process nucleosynthesis requires neutron heavy isotopes, and the two leading theories are neutron star mergers and type II supernovae (see references Burbridge 1957, Roberts 2010, Lattimer 1977). Even though the conditions of the neutron star environment are somewhat uncertain, estimates are promising for the neutron star mergers to produce heavy isotopes in r-process distributions. These two processes, neutron star mergers and type II supernovae are quite different in frequency and yields, meaning that galactic chemical evolution models should be able to predict which of the models are most likely.

2.2.5 neutron star merger application to `Eris`

Numerically, the neutron star mergers are described by delay-time distribution, merger rate, yield of r-process elements, and the spatial distribution of events. The delay-time distribution is modelled by a power-law, $P(t) \propto t^{-n}$, from some minimum timescale to the hubble-time(end of simulation). Each neutron star merger is assumed to synthesize some mass of r-process material, only a fraction of this material will be europium(which is used as the tracer). The ratio of europium to r-process material is usually assumed to be solar ($M_{Eu} = 9.3 \times 10^{-4} M_{r-process}$ Sneden 2008) , while the merger rate is calculated from scaling the star formation integral until europium-oxygen ratio equals solar ratio.

From the merger rate, the number of injection events per timestep is calculated and applied to random star particles in the data. The ejection material is then distributed among gas particles in close proximity to the selected star particles.

2.2.6 Chemical observations of Eris

At redshift zero the oxygen-iron abundances can be split into two main sources. One source is type II supernovae, which are more rich in oxygen, leading to higher (supersolar) ratios. Another source is type Ia supernovae, which are more rich in iron, leading to more iron than oxygen.

There are two main implementations of Eris postprocessing involved, one without any mixing, and another with mixing of metals between gas particles. For both oxygen-iron ratios and europium-iron ratios one sees that mixing gives less variation between "upper" and "lower" sigma-bands.

The chemical enrichment is closely tied to the star formation and evolution. Eris is a good approximation to the Milky Way galaxy do to similar star formation, shape and chemical composition today. *(Shen et al., 2015)* finds that neutron star mergers are capable of enriching the surrounding medium, even with a minimum delay-time of 100 Myr.

The dispersion of [Eu/Fe] is big enough, even at low metallicities, to reproduce the variations of observed europium in old low-mass stars. The mixing level affects the abundance of europium, but it is hard to compare to observations becasue spectroscopic abundance of many stars are unknown. The conclusion is that variations of the model parameters do not significantly alter the result.

Galactic chemical evolution models, like Omega, are single points in space with mass resolution and time-integration. These models are simple way of calculating the mean amount of elements in the galaxy based on a star formation history, yield tables and initial composition. These models do not replicate the inhomogeneities and variations in metal-distributions that are found in N-body simulations. *(Shen et al., 2015)* attempts to reproduce the results with a 1D-model based on the parameters found in Eris; At late times model agrees well with the average of all of Eris, however it does not agree well with the early results of Eris, nor does it replicate the large variations in spectroscopic abundance during early times.

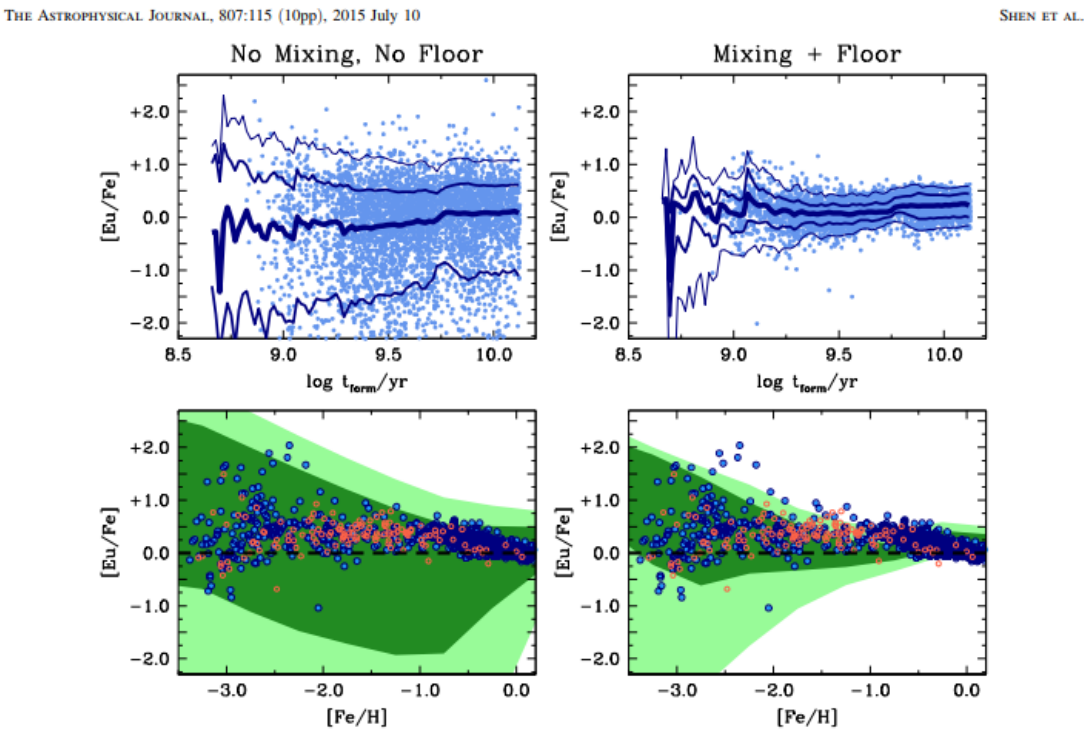

Figure 2.10: Top two panels show spectroscopic Eu in star particles against the formation time of said star particles. Time is shown in log-scale. The blue lines show mean, 68%, and 95% intervals of the stars. The bottom two panels show spectroscopic Eu in star particles relative to the iron abundance in said star particles. Dashed line represent the solar value, while shaded regions are the 68% and 95% intervals of the stellar data. All data is retrieved from a representative subsample of star particles at the end of the simulation (redshift zero).
The two left panels show the data from the `Eris`-simulation when there is no metallicity floor (a metallicity floor means that all particles have a minimum amount of metals at the beginning of the simulation, usually $10^{-4}\times$solar metallicity) and no mixing of metals between gas particles. On the two right panels, a metallicity floor and mixing of metals are implemented. This effect appears to lower the spread of metals in star particles at all times, and this result is consistent for iron and oxygen too *(Shen et al., 2015)* .
Plots and figures are taken from *(Shen et al., 2015, fig.4)*

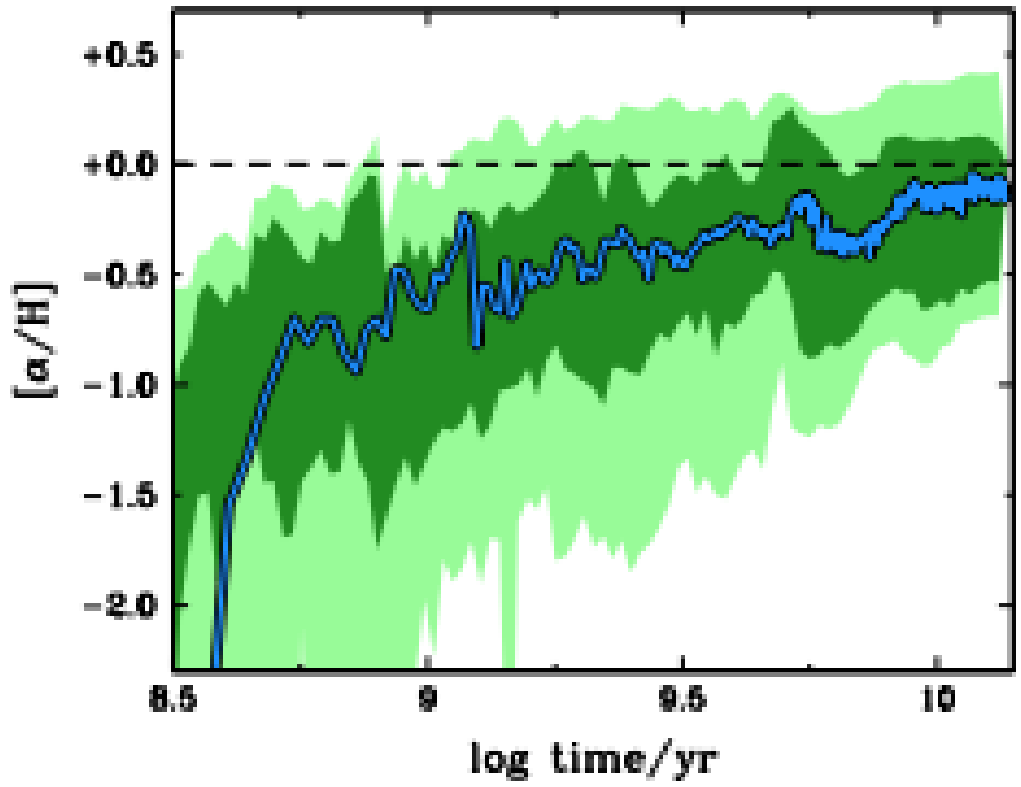
+0.5
+0.0
−0.5
−1.0
−1.5
−2.0
[α/H]
8.5
9
9.5
10
log time/yr

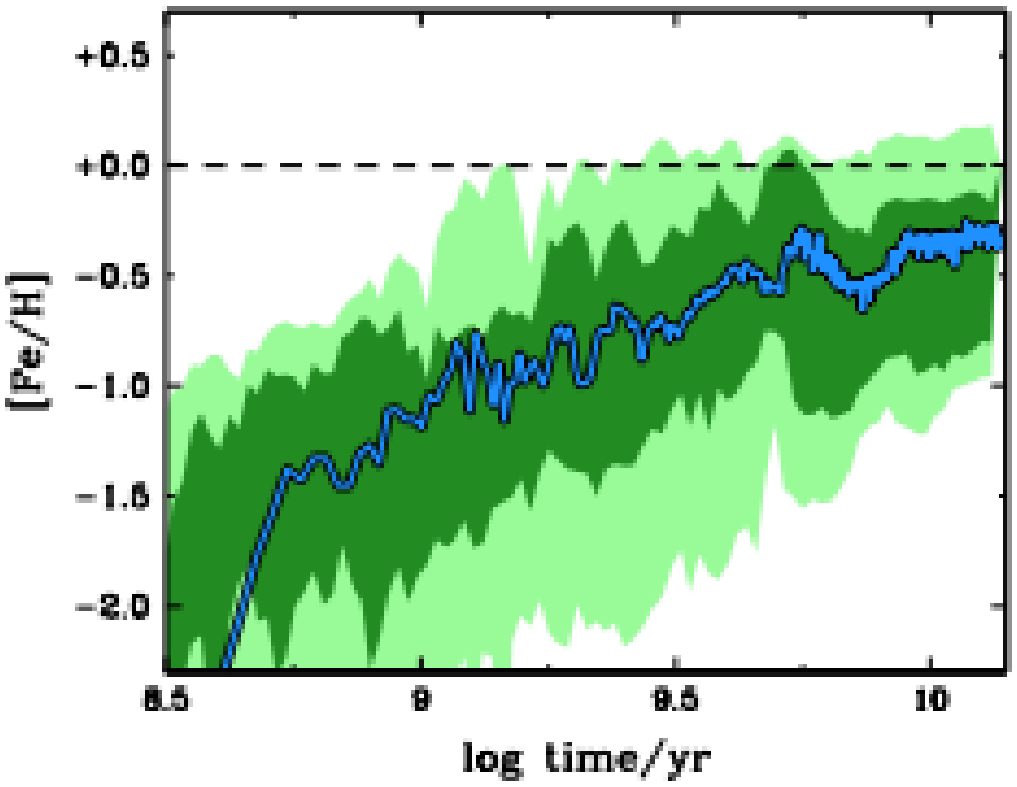
+0.5
+0.0
−0.5
−1.0
−1.5
−2.0
[Fe/H]
8.5
9
9.5
10
log time/yr

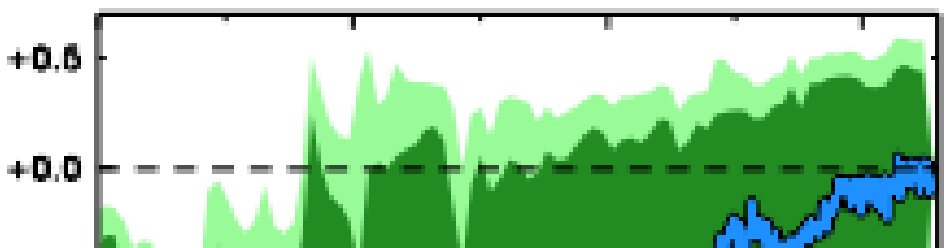
+0.5
+0.0

Bibliography

Cappellari, M., McDermid, R. M., Alatalo, K., et al. 2012, Nature, 484, 485

Chabrier, G. 2003, Publications of the Astronomical Society of the Pacific, 115, 763

Chiappini, C., Matteucci, F., & Romano, D. 2001, ApJ, 554, 1044

Côté, B., Ritter, C., O'Shea, B. W., et al. 2016, ApJ, 824, 82

Fuchs, B., Jahreiβ, H., & Flynn, C. 2009, The Astronomical Journal, 137, 266

Guedes, J., Callegari, S., Madau, P., & Mayer, L. 2011, ApJ, 742, 76

Heger, A., & Woosley, S. E. 2010, ApJ, 724, 341

Hirschi, R., Frischknecht, U., Pignatari, M., et al. 2008, in Nuclei in the Cosmos (NIC X)

Iwamoto, K., Brachwitz, F., Nomoto, K., et al. 1999, ApJS, 125, 439

Kroupa, P. 2001, Monthly Notices of the Royal Astronomical Society, 322, 231

Miller, G. E., & Scalo, J. M. 1979, The Astrophysical Journal Supplement Series, 41, 513

Monaghan, J. J. 1992, Annual Review of Astronomy and Astrophysics, 30, 543

Navarro, J. F., & Benz, W. 1991, ApJ, 380, 320

Salpeter, E. E. 1955, ApJ, 121, 161

Seitenzahl, I. R., Ciaraldi-Schoolmann, F., Röpke, F. K., et al. 2013, MNRAS, 429, 1156

Shen, S., Cooke, R. J., Ramirez-Ruiz, E., et al. 2015, ApJ, 807, 115

Thielemann, F.-K., Nomoto, K., & Yokoi, K. 1986, A&A, 158, 17

Thielemann, F.-K., Argast, D., Brachwitz, F., et al. 2003, in From Twilight to Highlight: The Physics of Supernovae, ed. W. Hillebrandt & B. Leibundgut, 331

Troja, E., Piro, L., van Eerten, H., et al. 2017, Nature, 551, 71

Wadsley, J. W., Stadel, J., & Quinn, T. 2004, New Astronomy, 9, 137